# Steady-state and Time-history Analyses for a Spatial Cable-driven Parallel Robot

Sy Nguyen-Van and Minh-Quang Tran

***Abstract*— Cable-driven parallel robots (CDPRs) are extremely flexible parallel manipulators, which have high velocity, acceleration, and payload to weight ratio compared with traditional rigid-link parallel robots. In this paper, the steady-state and time-history analyses of a spatial CDPR are developed using the finite element method (FEM) and the modified analytical method. To validate the feasibility of these two approaches in solving the steady-state and time-history responses of the spatial CDPR, the results from the proposed methods are examined with those of SAP2000®. It shows that their solutions are well fit to the results from SAP2000 which is time-consuming. This demonstrates the effectiveness of the FEM and the modified analytical method.**

***Index Terms*— *CDPRs, FEM, analytical method, steady-state response, time-history response***

## I. Introduction

Over the past decades, owing to the cutting-edge characteristics of cable-driven parallel robots (CDPR), this type has been received much interest from many scholars from all over the world. The CDPR is a category of parallel robots and uses flexible cables to connect the end-effector and the frame instead of using rigid links [1]. Thus, the end-effector is controlled by changing the length of the cable length [1]–[3]. Due to using such flexible cables, CDPRs have some noticeable advantages such as large reachable workspace, saving cost, lightweight, easy to assemble in various spatial configurations, and ease for transportation [3]–[8]. Hence, CDPRs have been used for applications in 3D printing [5], transportation [6], [9], and so on.

Although CDPRs have many interesting characteristics, they are facing a critical problem in terms of vibration because of using flexible cables. Indeed, cables are easily vibrated in both axial and transversal directions owning to their inevitably flexible characteristics [2]. Regarding vibration analysis of CDPRs, several approaches have been introduced to deal with that problem. In general, they can be categorized into four main groups: (1) the simple model by using spring elements, (2) the finite element approach, (3) the analytical method, and (4) the dynamic stiffness method.

This paper was first submitted on May 9, 2021.

Sy Nguyen-Van is with the Department of Mechanical Engineering, Thai Nguyen University of Technology, 3/2 Street, Tich Luong ward, Thai Nguyen, Vietnam. (e-mail: vansy@tnut.edu.vn).

Minh-Quang Tran is with the Industry 4.0 Implementation Center, Center for Cyber–physical System Innovation, National Taiwan University of Science and Technology, 10607 Taipei, Taiwan, and also with the Department of Mechanical Engineering, Thai Nguyen University of Technology, 3/2 Street, Tich Luong ward, Thai Nguyen, Vietnam (e-mail: minhquang.tran@mail.ntust.edu.tw).

Recently, Sy et al. [8] has been introduced a new finite element method and the modified analytical approach for modeling of cables in the CDPRs. These methods have been validated on free vibration analysis of planar and spatial CDPRs model. The natural frequencies of the CDPRs obtained by such two methods were validated by the results of SAP2000®. However, the steady-state and time-history analyses of CDPRs have not been investigated yet so far in such a study.

This paper aims to perform the steady-state and time-history analyses of CDPRs by using the above two methods (the finite element method and the modified analytical approach). For validations of their abilities in solving the steady-state and time-history analyses, the results of the proposed methods are validated using SAP2000.

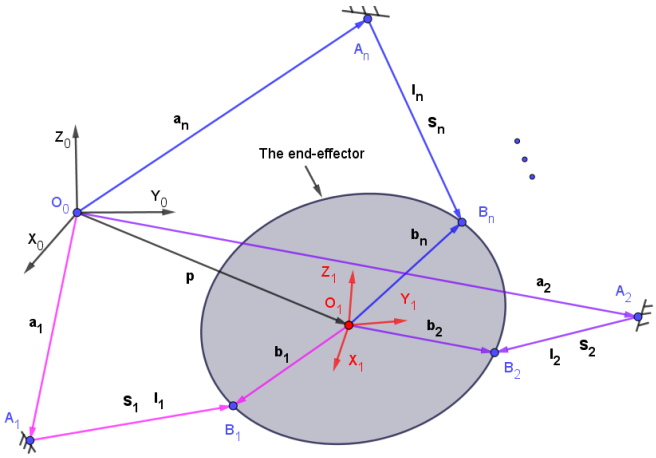


Figure 1. A general structure of cable robots [10].

## II. Dynamic Descriptions of Cable-driven Parallel Robots

As reported in [2], [8], for a general structure of cable-driven parallel robot shown in Figure 1, the kinematic equation for the CDPR is provided in Eq. (1),

$$\mathbf{p} = \mathbf{a}_i + \mathbf{l}_i - \mathbf{b}_i \qquad (i = 1, 2, ..., n) \tag{1}$$

where $\mathbf{l}_i$ is the vector along the $i^{th}$ cable and its norm is also the $i^{th}$ cable's length; $\mathbf{a}_i$, $\mathbf{b}_i$, and $\mathbf{p}$ present the position vectors of the point $A_i$, point $B_i$ and the centroid of the end-effector, respectively. $\boldsymbol{S}_i$ is the unit vector of the $i^{th}$ cable.

According to (1), the other kinematic equations are described by Eqs. (2)-(6),

$$\mathbf{l}_i^2 = [\mathbf{p} - \mathbf{a}_i + \mathbf{b}_i]^T [\mathbf{p} - \mathbf{a}_i + \mathbf{b}_i] \tag{2}$$

$$\dot{\mathbf{L}} = \mathbf{J}\mathbf{t} \tag{3}$$

$$\dot{\mathbf{L}} = [\dot{l}_1 \quad \dot{l}_2 \quad ... \quad \dot{l}_n]^T \tag{4}$$

$$\mathbf{J} = \begin{bmatrix} \mathbf{S}_1 & \mathbf{S}_2 & ... & \mathbf{S}_n \\ \mathbf{b}_1 \times \mathbf{S}_1 & \mathbf{b}_2 \times \mathbf{S}_2 & ... & \mathbf{b}_n \times \mathbf{S}_n \end{bmatrix}^T \tag{5}$$

$$\mathbf{t} = \begin{bmatrix} \dot{\mathbf{p}}^T \\ \boldsymbol{\omega}^T \end{bmatrix} \tag{6}$$

in which $\dot{\mathbf{p}}$ presents the linear velocity of the centroid and $\dot{\boldsymbol{\omega}}$ is the angular velocity of the end-effector. **J** presents the (*n* x *6*) Jacobian matrix of the CDPR. Thus, the dynamic equation of CDPRs is determined by Eq. (7) [2],

$$\begin{bmatrix} m\mathbf{I}_{3\times3} & \mathbf{0}_{3\times3} \\ \mathbf{0}_{3\times3} & \mathbf{I}_P \end{bmatrix} \begin{bmatrix} \ddot{\mathbf{p}} \\ \dot{\boldsymbol{\omega}} \end{bmatrix} + \begin{bmatrix} \mathbf{0}_{3\times1} \\ \boldsymbol{\omega} \times \mathbf{I}_P \times \boldsymbol{\omega} \end{bmatrix} + \begin{bmatrix} -m\mathbf{g} \\ \mathbf{0}_{3\times1} \end{bmatrix} + \begin{bmatrix} \mathbf{f}_e \\ \boldsymbol{\tau}_e \end{bmatrix} = \mathbf{J}^T\mathbf{T} \tag{7}$$

where *m* stands for the mass of the end-effector; $\mathbf{I}_P$ presents the inertia tensor of the end-effector about its centroid corresponding to the global frame $O_0$; $\mathbf{I}_{3x3}$ is the 3x3 identity matrix; **g** is the gravity acceleration vector; $\mathbf{f}_e$ presents the applied force vector; and $\boldsymbol{\tau}_e$ is the applied moment vector of the end-effector; **T** is the force vector of the cable, $\mathbf{T} = [T_1 \quad T_2 \quad ... \quad T_n]$. Hence, the force vector of the cable is determined by Eq. (8),

$$\mathbf{J}^T\mathbf{T} = \mathbf{w} \tag{8}$$

where **w** is the applied wrench and is defined using Eq. (9),

$$\mathbf{w} = \begin{bmatrix} -m\mathbf{g} \\ \mathbf{0}_{3\times1} \end{bmatrix} + \begin{bmatrix} \mathbf{f}_e \\ \boldsymbol{\tau}_e \end{bmatrix} \tag{9}$$

It should be noted that tensions applied to cables are calculated by the tension distribution algorithm. In this work, the quadratic or nonlinear programming algorithm is proposed to define the tension applied to cables which are described by Eqs. (10)-(12),

$$\text{minimize:} \frac{1}{2}\mathbf{T}^T\mathbf{C}\mathbf{T} + \mathbf{c}^T\mathbf{T} \tag{10}$$

$$\text{with:} T_{\min} \le T_i \le T_{\max} \tag{11}$$

$$\mathbf{J}^T\mathbf{T} = \mathbf{w} \tag{12}$$

where **C** and **c** denote the weighting factor of the objective function, respectively. $T_{max}$ and $T_{min}$ denote the maximum and the minimum tension allowed to cables, respectively.

## III. FINITE ELEMENT FORMULATION

Regarding a cable element that contains nodes of *i* and *j*, has the length of $l_{ij}$, it is applied a tension of $T_{ij}$. Thus, the general equation of motion of an element on the cable is described in Eq. (13) [8], [11], [12].

$$\mathbf{M}\ddot{\mathbf{u}} + (\mathbf{K}_L + \mathbf{K}_G)\mathbf{u} = \mathbf{0} \tag{13}$$

where $\mathbf{u}$ is the displacement and $\ddot{\mathbf{u}}$ is the acceleration vector. While $\mathbf{K}_L$ presents the conventional stiffness matrix and $\mathbf{K}_G$ describes the geometric stiffness matrix. Those parameters are defined in Eq. (14),

$$\mathbf{u} = \begin{bmatrix} u_{xi} & u_{yi} & u_{zi} & u_{xj} & u_{yj} & u_{zj} \end{bmatrix}^T \tag{14a}$$

$$\mathbf{K}_L = \int_0^1 (k_s - T_{ij}) l_{ij} \left( \mathbf{N}'^T \mathbf{N}' \boldsymbol{\Delta}\boldsymbol{\Delta}^T \mathbf{N}'^T \mathbf{N}' \right) d\xi \tag{14b}$$

$$\mathbf{K}_G = \int_0^1 T_{ij} l_{ij} \mathbf{N}' d\xi \tag{14c}$$

$$\boldsymbol{\Delta} = \begin{bmatrix} x_i & y_i & z_i & x_j & y_j & z_j \end{bmatrix}^T \tag{14d}$$

where **N** denotes for the shape function; **N'** stands for the ordinary differentiation of the shape function ( **N** ); $k_s$ is the elastic stiffness with $k_s = EA$; $\zeta = x / l_{ij}$ has a value in the range [0, 1]; $\boldsymbol{\Delta}$ denotes for the vector of nodal coordinates. Then, **N** and **N'** are given as follows.

$$\mathbf{N} = \begin{bmatrix} (1-\xi)\mathbf{I} & \xi\mathbf{I} \end{bmatrix}; \mathbf{N}' = \frac{1}{l_{ij}} \begin{bmatrix} -\mathbf{I} & \mathbf{I} \end{bmatrix} \tag{15}$$

where **I** is the (3x3) unit matrix, thus Eq. (15) can be rewritten by Eq. (16).

$$\mathbf{N}'^T\mathbf{N}' = \frac{1}{l_{ij}^2} \begin{bmatrix} \mathbf{I} & -\mathbf{I} \\ -\mathbf{I} & \mathbf{I} \end{bmatrix} \tag{16}$$

The mass matrix **M** is defined by Eq. (17),

$$\mathbf{M} = \frac{\gamma l_{ij}}{6g} \begin{bmatrix} 2\mathbf{I} & \mathbf{I} \\ \mathbf{I} & 2\mathbf{I} \end{bmatrix} \tag{17}$$

where $\gamma$ stands for the weight per unit length. Hence, the stiffness matrix is presented in Eqs. (18),

$$\mathbf{K}_L = \frac{k_s - T_{ij}}{l_{ij}} \begin{bmatrix} \mathbf{G} & -\mathbf{G} \\ -\mathbf{G} & \mathbf{G} \end{bmatrix} \tag{18a}$$

$$\mathbf{K}_G = \frac{T_{ij}}{l_{ij}} \begin{bmatrix} \mathbf{I} & -\mathbf{I} \\ -\mathbf{I} & \mathbf{I} \end{bmatrix} \tag{18b}$$

where **G** is the transformation matrix and it is calculated by Eqs. (19),

$$\mathbf{G} = \begin{bmatrix} l^2 & ml & nl \\ ml & m^2 & nm \\ nl & nm & n^2 \end{bmatrix} \tag{19a}$$

$$l=(x_j-x_i)/l_{ij};m=(y_j-y_i)/l_{ij};n=(z_j-z_i)/l_{ij} \tag{19b}$$

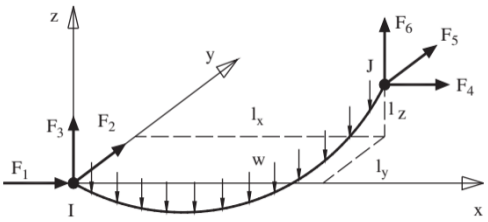


Figure 2. The three-dimensional catenary cable element [13].

## IV. THE MODIFIED ANALYTICAL METHOD

Figure 2 illustrates a cable element, in which the two nodes of the cable are *I(0,0,0)* and *J*($l_x$, $l_y$, $l_z$). *s* and *p* stand for the undeformed and deformed configurations of the cable element, respectively. Hence, the three equilibrium equations of the cable element are described in Eqs. (20),

$$T\left(\frac{dx}{dp}\right)=-F_1 \tag{20a}$$

$$T\left(\frac{dy}{dp}\right)=-F_2 \tag{20b}$$

$$T\left(\frac{dz}{dp}\right)=-F_3+\gamma s \tag{20c}$$

where, $F_1$, $F_2$, $F_3$ are the cable tension components projected in *x*-, *y*-and *z*-axis, respectively; γ presents the weight per unit length of the cable; *T* denotes the cable tension applied at the Lagrange coordinate *s*. In CDPRs, *T* is generated by using the tension distribution algorithm in Section II. The relationship between T and $F_1$, $F_2$, $F_3$ is given as follows:

$$T(s)=\sqrt{F_1^{\,2}+F_2^{\,2}+(F_3-\gamma s)^2} \tag{21}$$

Also, the tension (*T*) and the strain (ε) of the cable element has a relationship as follows:

$$T=EA\varepsilon=EA\left(\frac{dp-ds}{ds}\right)=EA\left(\frac{dp}{ds}-1\right) \tag{22}$$

where *E* stands for Young's modulus, *A* denotes the cross-sectional area of the cable element.

The Cartesian coordinates are presented in terms of the Lagrange coordinate of *s* in Eqs. (23),

$$x=\int_0^L\frac{dx}{ds}ds=\int_0^L\frac{dx}{dp}\frac{dp}{ds}ds \tag{23a}$$

$$y=\int_0^L\frac{dy}{ds}ds=\int_0^L\frac{dy}{dp}\frac{dp}{ds}ds \tag{23b}$$

$$z=\int_0^L\frac{dz}{ds}ds=\int_0^L\frac{dz}{dp}\frac{dp}{ds}ds \tag{23c}$$

As shown in **Error! Reference source not found.**, six boundary conditions are described in Eqs. (24),

$$x(0)=y(0)=z(0) \tag{24a}$$

$$x(L_0)=l_x,y(L_0)=l_y,z(L_0)=l_z \tag{24b}$$

By substituting Eqs. (20-22) into Eq.(23), the cable lengths are projected in x-, y-and z-direction using Eqs. (25),

$$\begin{aligned}l_x=&-\frac{F_1L_0}{EA}-\frac{F_1}{\gamma}\{\ln\left[\sqrt{F_1^{\,2}+F_2^{\,2}+(-F_3+\gamma L_0)^2}\right]+\\&+\gamma L_0-F_0-\ln\left(\sqrt{F_1^{\,2}+F_2^{\,2}+F_3^{\,2}}-F_3\right)\}\end{aligned} \tag{25a}$$

$$\begin{aligned}l_y=&-\frac{F_2L_0}{EA}-\frac{F_2}{\gamma}\{\ln\left[\sqrt{F_1^{\,2}+F_2^{\,2}+(-F_3+\gamma L_0)^2}\right]+\\&+\gamma L_0-F_0-\ln\left(\sqrt{F_1^{\,2}+F_2^{\,2}+F_3^{\,2}}-F_3\right)\}\end{aligned} \tag{25b}$$

$$\begin{aligned}l_z=&-\frac{F_3L_0}{EA}+\frac{\gamma L_0^2}{2EA}+\\&+\frac{1}{\gamma}\left[\sqrt{F_1^{\,2}+F_2^{\,2}+(-F_3+\gamma L_0)^2}-\sqrt{F_1^{\,2}+F_2^{\,2}+F_3^{\,2}}\right]\end{aligned} \tag{25c}$$

where $L_0$ presents the unstressed length of the cable. Then, the above Eqs. (25) can be expressed in terms of the node forces ($F_1,F_2,F_3$) as follows:

$$l_x=f(F_1,F_2,F_3) \tag{26a}$$

$$l_y=g(F_1,F_2,F_3) \tag{26b}$$

$$l_z=h(F_1,F_2,F_3) \tag{26c}$$

The above equations are differentiated to $F_1,F_2,F_3$, as follows:

$$dl_x=\frac{\partial f}{\partial F_1}dF_1+\frac{\partial f}{\partial F_2}dF_2+\frac{\partial f}{\partial F_3}dF_3 \tag{27a}$$

$$dl_y=\frac{\partial g}{\partial F_1}dF_1+\frac{\partial g}{\partial F_2}dF_2+\frac{\partial g}{\partial F_3}dF_3 \tag{27b}$$

$$dl_z=\frac{\partial h}{\partial F_1}dF_1+\frac{\partial h}{\partial F_2}dF_2+\frac{\partial h}{\partial F_3}dF_3 \tag{27c}$$

Writing into a matrix form as following Eq. (28),

$$\begin{bmatrix}dl_x\\dl_y\\dl_z\end{bmatrix}=\begin{bmatrix}f_{11}&f_{12}&f_{13}\\f_{21}&f_{22}&f_{23}\\f_{31}&f_{32}&f_{33}\end{bmatrix}\begin{bmatrix}dF_1\\dF_2\\dF_3\end{bmatrix}=F\begin{bmatrix}dF_1\\dF_2\\dF_3\end{bmatrix} \tag{28}$$

where *F* presents the flexibility matrix. All elements of matrix $f_{ij}$ are described in Eq. (29),

$$f_{11} = -\left(\frac{L_0}{EA} + \frac{1}{\gamma}\log\frac{T_j + F_6}{T_i - F_3}\right) + \\ + \frac{F_1^2}{\gamma}\left[\frac{1}{T_i(T_i - F_3)} - \frac{1}{T_j(T_j + F_6)}\right] \quad (29a)$$

$$f_{12} = f_{21} = \frac{F_1 F_2}{\gamma}\left[\frac{1}{T_i(T_i - F_3)} - \frac{1}{T_j(T_j + F_6)}\right] \\ f_{13} = f_{31} = \frac{F_1}{\gamma}\left[\frac{1}{T_j} - \frac{1}{T_i}\right] \quad (29b)$$

$$f_{22} = -\left(\frac{L_0}{EA} + \frac{1}{\gamma}\log\frac{T_j + F_6}{T_i - F_3}\right) + \\ + \frac{F_2^2}{\gamma}\left[\frac{1}{T_i(T_i - F_3)} - \frac{1}{T_j(T_j + F_6)}\right] \quad (29c)$$

$$f_{23} = f_{32} = \frac{F_2}{\gamma}\left[\frac{1}{T_i} - \frac{1}{T_j}\right] \\ f_{33} = -\frac{L_0}{EA} - \frac{1}{\gamma}\left[\frac{F_6}{T_j} + \frac{F_3}{T_i}\right] \quad (29d)$$

with $T_i$ and $T_j$ are initial tensions applied to the cable robots:

$$T_i = \sqrt{F_1^2 + F_2^2 + F_3^2} \quad (30a)$$

$$T_j = \sqrt{F_4^2 + F_5^2 + F_6^2} \quad (30b)$$

where,

$$F_4 = -F_1 \quad (31a)$$

$$F_5 = -F_2 \quad (31b)$$

$$F_6 = -F_3 + \gamma L_0 \quad (31c)$$

Finally, the stiffness and the tangent stiffness matrix are calculated using Eqs. (32) and (33),

$$\mathbf{K} = \mathbf{F}^{-1} = \begin{bmatrix} f_{11} & f_{12} & f_{13} \\ f_{21} & f_{22} & f_{23} \\ f_{31} & f_{32} & f_{33} \end{bmatrix}^{-1} \quad (32)$$

$$\mathbf{K}_T = \begin{bmatrix} -\mathbf{K} & \mathbf{K} \\ \mathbf{K} & -\mathbf{K} \end{bmatrix} \quad (33)$$

In this paper, the applied cable tensions ($T_0$) in the modified analytical formulation are calculated by the tension distribution algorithm described in Section 2 for the CDPRs. Then, the stiffness matrix of cables can be generated using the following procedure:

- *Step 1:* Input *w, E, A* and nodes $I(x_i, y_i, z_i)$, $J(x_j, y_j, z_j)$.
- *Step 2:* Calculate $l_{x0} = x_j - x_i, l_{y0} = y_j - y_i, l_{z0} = z_j - z_i$.
- *Step 3:* Initializing the values of $L_0$, $F_1$, $F_2$, $F_3$.

$$L_0 = \sqrt{{l_{x0}}^2 + {l_{y0}}^2 + {l_{z0}}^2}$$

$$F_1 = -\frac{l_{x0}}{L_0}T_0$$

$$F_2 = -\frac{l_{y0}}{L_0}T_0$$

$$F_3 = -\frac{l_{z0}}{L_0}T_0$$

- *Step 4:* Calculate $T_i$ and $T_j$ using Eq. (30a) and Eq. (30b).
- *Step 5:* Determine the stiffness matrix using Eq. (32) and Eq. (33).

The Newton Raphson iteration for updating the misclosure vector is not considered in this modified procedure: $dL = \{(l_{xo} - l_x) \ \ (l_{yo} - l_y) \ \ (l_{zo} - l_z)\}^T$ . Thus, this algorithm can model perfectly vertical cables.

## V. DYNAMIC RESPONSES

In this section, the formulations of the steady-state and time history analyses are presented first then numerical simulations of a spatial CDPR are performed. It should be noted that some assumptions for modeling of the CDPR are made as follows:

- The total mass of the platform is the point mass located at the centroid of the end-effector.
- All cables are connected at the centroid of the end-effector.
- Cable tensions are determined by using the tension distribution algorithms mentioned in Section 2.

### *A. Steady-state response*

For general vibration models of CDPRs, its dynamic equation describes in Eq. (34).

$$\mathbf{M}\ddot{\mathbf{u}} + \mathbf{K}\mathbf{u} = \mathbf{F_0}e^{\omega t} \quad (34)$$

where, the frequency and amplitude of the excitation force are $\omega$ and $F_0$, respectively. The displacement and the acceleration vectors are $u$ and $\ddot{u}$ , respectively.

$$\mathbf{u} = \mathbf{A}e^{\omega t} \quad (35)$$

$$\ddot{\mathbf{u}} = \boldsymbol{\omega}^2\mathbf{A}e^{\omega t} \quad (36)$$

where $A$ is the amplitude of the displacement response. Substituting $u$ and $\ddot{u}$ into Eq.(34), we can get:

$$\left(\mathbf{K} - \omega^2\mathbf{M}\right)\mathbf{A} = \mathbf{F_0} \quad (37)$$

The amplitude in terms of the frequency of the excitation force is given as follows:

$$\mathbf{A}(\omega) = \left[\mathbf{K} - \omega^2\mathbf{M}\right]^{-1}\mathbf{F_0} \quad (38)$$

Then, the frequency response function is defined as follows:

$$\mathbf{H}(\omega) = \log_{10}\left[\mathbf{A}(\omega)\right] \tag{39}$$

*B. The Newmark-Beta method*

One of the most famous algorithms to solve the time history dynamic response of the structures is the Newmark-Beta method [13]. The general dynamic equation of motions of cable structures is defined by Eq. (40).

$$\mathbf{M}\ddot{\mathbf{u}}(t) + \mathbf{C}\dot{\mathbf{u}}(t) + \mathbf{K}\mathbf{u}(t) = \mathbf{F}(t) \tag{40}$$

where **M**, **C,** and **K** represent the mass matrix, damping matrix, and stiffness matrix, respectively; **F**(t) is the external applied load's vector; while $\ddot{\mathbf{u}}(t), \dot{\mathbf{u}}(t)$ and $\mathbf{u}(t)$ are the acceleration vector, velocity vector, and displacement vector, respectively.

The damping matrix can be calculated as follows:

$$\mathbf{C} = \delta_M \mathbf{M} + \delta_K \mathbf{K} \tag{41}$$

in which $\delta_M$ and $\delta_K$ present mass and stiffness proportional damping factors, respectively, and their values are both equal to 0.05 [14]. To solve the dynamic equation with known external forces, the initial acceleration, velocity, and displacement, the Newmark-beta method is applied to get the total dynamic response in terms of time.

A proposed procedure to determine the dynamic response for the spatial CDPR is as follows:

*Step1: Initial calculations*

a. Defining the stiffness-matrix **K**, the mass-matrix **M**, and the damping constant C.

b. Initializing ${}^{0}\ddot{\mathbf{u}}, {}^{0}\dot{\mathbf{u}}$ *and* ${}^{0}\mathbf{u}$ (the initial acceleration, velocity, and displacement)

$$\mathbf{M}_0\ddot{\mathbf{u}}_0 + \mathbf{C}_0\dot{\mathbf{u}}_0 + \mathbf{K}_0\mathbf{u}_0 = \mathbf{F}_0 \tag{42}$$

$$\ddot{\mathbf{u}}_0 = \mathbf{M}_0^{-1}\left(\mathbf{F}_0 - \mathbf{C}_0\dot{\mathbf{u}}_0 - \mathbf{K}_0\mathbf{u}_0\right) \tag{43}$$

c. Selecting time step $\Delta t$ and parameters $\alpha$ and $\beta$, then calculating integration constants:

$$\alpha \geq 0.50, \qquad \beta \leq \frac{\alpha}{2} \tag{44}$$

$$\begin{aligned} &a_0 = \frac{1}{\beta\Delta t^2}; a_1 = \frac{\alpha}{\beta\Delta t}; a_2 = \frac{1}{\beta\Delta t}; \\ &a_3 = \frac{1}{2\beta} - 1; a_4 = \frac{\alpha}{\beta} - 1; a_5 = \frac{\Delta t}{2}\left(\frac{\alpha}{\beta} - 2\right); \\ &a_6 = \Delta t(1-\alpha); \qquad a_7 = \alpha\Delta t \end{aligned} \tag{45}$$

d. Determining effective stiffness matrix $\hat{\mathbf{K}}$:

$$\hat{\mathbf{K}} = \mathbf{K} + a_0\mathbf{M} + a_1\mathbf{C} \tag{46}$$

*Step 2: For each time step*

a. Calculate effective loads at the time $t + \Delta t$:

$$\begin{aligned} {}^{t+\Delta t}\hat{\mathbf{F}} = {}^{t+\Delta t}\mathbf{F} + \mathbf{M}(a_0\,{}^{t}\mathbf{u} + a_2\,{}^{t}\dot{\mathbf{u}} + a_3\,{}^{t}\ddot{\mathbf{u}}) + \\ +\mathbf{C}(a_1\,{}^{t}\mathbf{u} + a_4\,{}^{t}\dot{\mathbf{u}} + a_5\,{}^{t}\ddot{\mathbf{u}}) \end{aligned} \tag{47}$$

b. Solve for the displacement at the time $t + \Delta t$:

$$\hat{\mathbf{K}}\,{}^{t+\Delta t}\mathbf{u} = {}^{t+\Delta t}\hat{\mathbf{F}} \tag{48}$$

c. Determine accelerations and velocities at the time $t + \Delta t$:

$${}^{t+\Delta t}\ddot{\mathbf{u}} = a_0({}^{t+\Delta t}\mathbf{u} - {}^{t}\mathbf{u}) - a_2\,{}^{t}\dot{\mathbf{u}} - a_3\,{}^{t}\ddot{\mathbf{u}} \tag{49}$$

$${}^{t+\Delta t}\dot{\mathbf{u}} = {}^{t}\dot{\mathbf{u}} + a_6\,{}^{t}\ddot{\mathbf{u}} + a_7\,{}^{t+\Delta t}\ddot{\mathbf{u}} \tag{50}$$

*C. Numerical simulations*

In this section, a spatial CDPR in Figure 3 which is exerted by a harmonic force is performed for the steady-state and time-history responses. In this scheme, $T_i$ and $A_i$ stand for the applied tension and the cross-sectional area of the $i^{th}$ cable. Data for the simulations of the spatial CDPR are listed in Table 1.

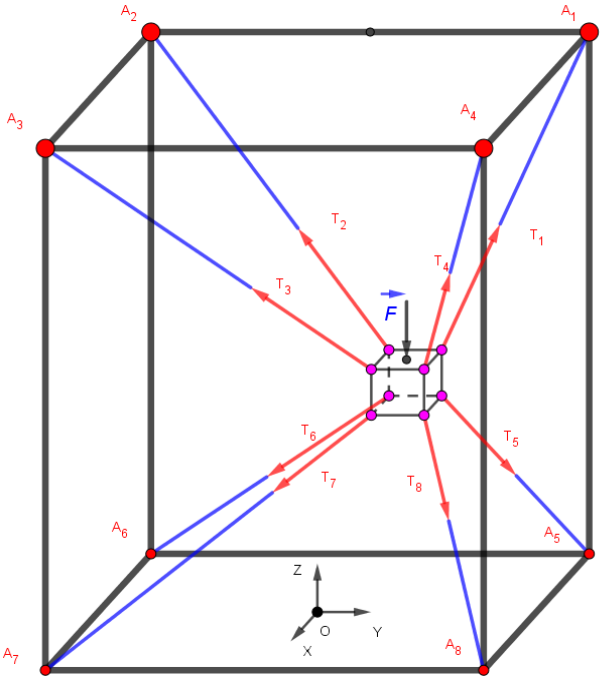


Figure 3. The CDPR exerted by the harmonic force.

TABLE 1
PARAMETER DESCRIPTIONS OF A SPATIAL CABLE-DRIVEN PARALLEL ROBOT

| **Parameter descriptions** | **Value** |
|---|---|
| The end-effector mass *(kg)* | 30 |
| The cross-sectional areas' *A* ($m^2$) | 50.265 x $10^{-6}$ |
| The frame dimensions of the CDPR *(m)* | 2.5 x 2.5 x 2.5 |
| The of end-effector position, *[x,y,z] (m)* | [0;0;1.25] |
| The elasticity modulus, *E*($N/m^2$) | 2.01 x $10^{10}$ |
| The weight per unit length, $\gamma$ *(N/m)* | 0.251 |
| The minimum tension, $T_{min}$ *(N)* | 100 |
| The maximum tension, $T_{max}$ *(N)* | 1000 |

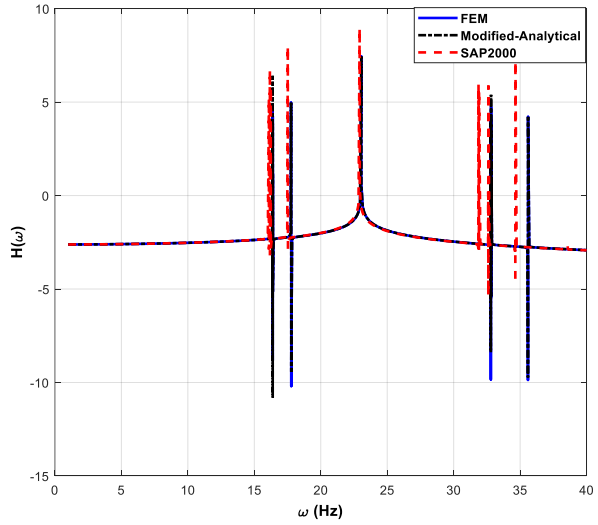


Figure 4. The frequency response of the CDPR.

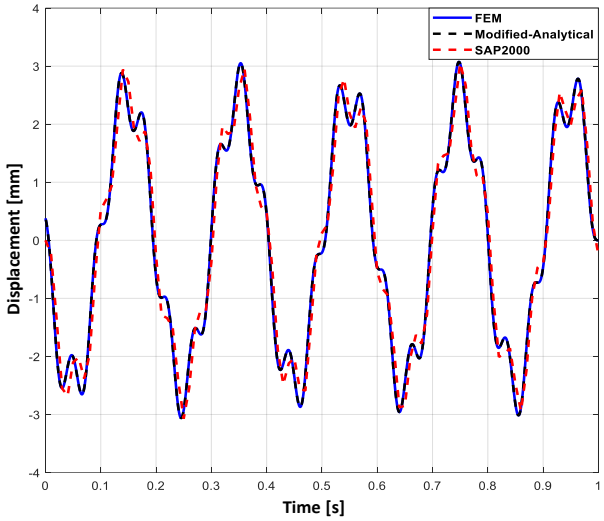


Figure 5. The dynamic response vibration of the CDPR

*1) Steady-state response*

Regarding the CDPR in Figure 3, the amplitude of the external force of 1500 N is applied to the end-effector along the z-axis and the range of excitation frequency is from 1 Hz to 40 Hz with 390 equal steps. The frequency response of the cable-driven parallel robot is illustrated in Figure 4. It shows that the frequency response gotten from the FEM, modified analytical models are nearly identical to the response of SAP2000. Thus, the FEM and modified analytical models of the CDPR can accurately predict the steady-state response.

*2) Time history response*

The parameters of Newmark, $[\alpha,\beta]$, are also [0.5, 0.25], respectively. The harmonic external force is applied to the end-effector along the z-axis with an amplitude $F_0$, and the excitation frequency, $f_C$, of 5 Hz. The time of analysis is 1 second (s) and the time step is 0.001s. The horizontal

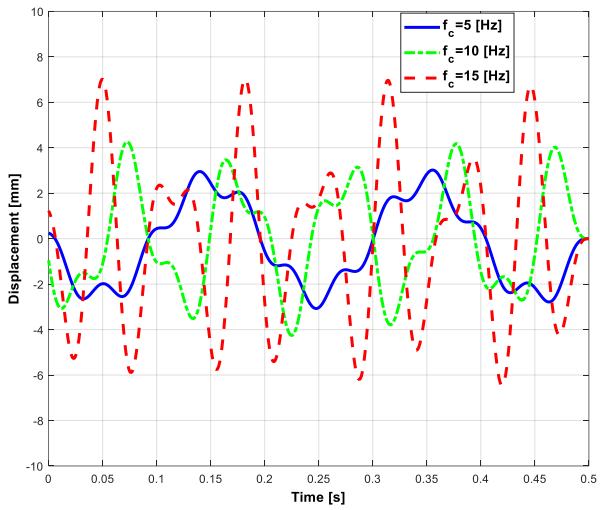


Figure 6. The z-response of the end-effector of the CDPR according to excitation frequencies.

displacement responses of the end-effector due to the harmonic external force gotten by the FEM, modified analytical method, and SAP2000 are shown in Figure 5. It can be seen that a good agreement of displacement responses of the end-effector gotten by FEM and modified analytical in this research and SAP2000 is obtained.

In addition, Figure 6 illustrates the displacement responses of the end-effector obtained by FEM in 0.5 seconds corresponding to three differential frequencies (5 Hz, 10 Hz and 15 Hz) of the harmonic force (F with the amplitude of F0). Although the amplitude $F_0$ is not changed, the magnitude of response is increased by increasing the frequency of the external forces.

## VI. Conclusion

In this paper, the steady-state and time history dynamic responses of the spatial CDPR were presented using the FEM and the modified analytical method. The proposed approaches were verified in terms of accuracy compared to those of SAP2000. Excellent results obtained proposed methods demonstrate that the dynamic behaviors of CDPR can be achieved by using FEM and the modified analytical method instead of using time-consuming software such as SAP2000. Consequently, some conclusions can be made as follows:

- With different excitation frequencies and the same amplitudes of harmonic forces, the displacement responses of the end-effector in the CDPR will have different amplitudes.
- These results prove that the developed FEM and the modified analytical method can be effectively used in the preliminary design of the CDPR.

## Acknowledgment

This research is supported by Thai Nguyen University of Technology in Vietnam and the Center for Cyber-physical System Innovation at Taiwan Tech in Taiwan.

## REFERENCES

[1] M. A. Khosravi and H. D. Taghirad, "Robust PID control of fully-constrained cable driven parallel robots," *Mechatronics*, vol. 24, no. 2, pp. 87–97, 2014, [Online]. Available: http://www.sciencedirect.com/science/article/pii/S0957415813002353.

[2] X. Diao and O. Ma, "Vibration analysis of cable-driven parallel manipulators," *Multibody Syst. Dyn.*, vol. 21, no. 4, pp. 347–360, 2009.

[3] H. Yuan, E. Courteille, and D. Deblaise, "Static and dynamic stiffness analyses of cable-driven parallel robots with non-negligible cable mass and elasticity," *Mech. Mach. Theory*, vol. 85, pp. 64–81, 2015, doi: 10.1016/j.mechmachtheory.2014.10.010.

[4] X. Zhang *et al.*, "Large-scale 3D printing by a team of mobile robots," *Autom. Constr.*, vol. 95, pp. 98–106, 2018, doi: 10.1016/j.autcon.2018.08.004.

[5] E. Barnett and C. Gosselin, "Large-scale 3D printing with a cable-suspended robot," *Addit. Manuf.*, vol. 7, pp. 27–44, 2015.

[6] A. Pott, *Cable-Driven Parallel Robots: Theory and Application*. Springer International Publishing, 2018.

[7] S. Nguyen-Van, D. T. T. Thuy, N. N. T. Thanh, and N. N. Dinh, "Evolutionary Tuning of PID Controllers for a Spatial Cable-Driven Parallel Robot BT -," in *Advances in Engineering Research and Application*, 2021, pp. 411–424.

[8] S. Nguyen-Van, K. W. Gwak, D. H. Nguyen, S. G. Lee, and B. H. Kang, "A novel modified analytical method and finite element method for vibration analysis of cable-driven parallel robots," *J. Mech. Sci. Technol.*, no. September, 2020, doi: 10.1007/s12206-020-0809-9.

[9] J. U. and J. D. L. N. G. Dagalakis, J. S. Albus, B.-L. Wang, "Stiffness Study of a Parallel Link Robot Crane for Shipbuilding Applications," *J. Offshore Mech. Arct. Eng.*, vol. 111, no. 3, pp. 183–193, 1989.

[10] R. Babaghasabha, M. A. Khosravi, and H. D. Taghirad, "Robust PID control of fully-constrained cable driven parallel robots," *Mechatronics*, vol. 24, no. 2, pp. 87–97, 2014.

[11] M. L. Gambhir and B. de V. Batchelor, "Finite element study of the free vibration of 3-D cable networks," *Int. J. Solids Struct.*, vol. 15, no. 2, pp. 127–136, 1979.

[12] H. Ozdemir, "A finite element approach for cable problems," *Int. J. Solids Struct.*, vol. 15, no. 5, pp. 427–437, 1979, doi: 10.1016/0020-7683(79)90063-5.

[13] H. T. Thai and S. E. Kim, "Nonlinear static and dynamic analysis of cable structures," *Finite Elem. Anal. Des.*, vol. 47, no. 3, pp. 237–246, 2011, [Online]. Available: http://dx.doi.org/10.1016/j.finel.2010.10.005.

[14] Junuthula N. Reddy, *An Introduction to the Finite Element Method*. McGraw-Hill Education, 2005.